International Journal of Heat and Mass Transfer 52 (2009) 516–524

Contents lists available at ScienceDirect

International Journal of Heat and Mass Transfer

journal homepage: www.elsevier.com/locate/ijhmt

A new generation cooling device employing $CaCl_2$-in-silica gel–water system

Bidyut Baran Saha [a,*], Anutosh Chakraborty [a], Shigeru Koyama [a], Yu I. Aristov [b]

[a] Interdisciplinary Graduate School of Engineering Sciences, Kyushu University, 6-1 Kasuga-Koen, Kasuga-Shi, Fukuoka 816-8580, Japan
[b] Boreskov Institute of Catalysis, Siberian Division, Russian Academy of Sciences, pr. Akademika Lavrent'eva 5, Novosibirsk 630090, Russia

ARTICLE INFO

Article history:
Received 16 November 2007
Available online 19 August 2008

Keywords:
Adsorption
Cooling
$CaCl_2$-in-silica gel
Silica gel
Waste heat recovery

ABSTRACT

This article presents the dynamic modelling of a single effect two-bed adsorption chiller utilizing the composite adsorbent "$CaCl_2$ confined to KSK silica gel" as adsorbent and water as adsorbate, which is based on the experimentally confirmed adsorption isotherms and kinetics data. Compared with the experimental data of conventional adsorption chiller based on RD silica gel + water pair, we found that the new working pair provides better cooling capacity and performances. From numerical simulation, it is also found that the cooling capacity can be increased up to 20% of the parent silica gel + water adsorption chiller and the coefficient of performance (COP) can be improved up to 25% at optimum conditions. We also demonstrate here that the best peak chilled water temperature suppression, and the maximum cooling capacity can be achieved by the optimum analysis for both cycles.

1. Introduction

The development of adsorption cooling system is based on the thermal compression of natural working refrigerants like water or alcohols and lies in its ability to operate with motive energy derived from fairly low temperature sources such as waste heat in process industries or sun light which indicates the adsorption process as an avenue for avoiding the use of ozone depleting substances [1]. The widespread acceptance of the adsorption systems is hindered by its relatively poor performances and large size due to limited properties of solid adsorbents. Principal advantage of adsorption chillers (ADCs) is that it is amenable to regenerative use of adsorption heat. Adsorption system incorporates no mechanical moving parts and generates no noise or vibration.

It should be noted here that the performance of ADC depends largely on the adsorption isotherms, kinetics and the isosteric heat of adsorption of adsorbent–refrigerant pair. A review of literature reveals that numerous investigations are reported on various adsorption system configurations, experimental investigations and mathematical modelling of the steady state and transient behavior of adsorption cycles [2–4]. A certain number of adsorbent–adsorbate pairs have been tested theoretically and experimentally for evaluating the performances of ADCs. These are silica gel + water, zeolite + water, silica gel + methanol, activated carbon + methanol, activated charcoal + NH_3, zeolite + CO_2, etc., and a literature review of these pairs [5–32] is furnished in Table 1. This table demonstrates that the Freundlich, Tóth, Dubinin–Astakhov, Dubinin–Radushkevich equations are mainly used for describing the equilibrium adsorption. The heat of adsorption is derived from the isosteric chart of adsorbent–adsorbate pair presented in the Clapeyron coordinates. Adsorption kinetics is approximated by the linear driving force (LDF) model suggested for analyzing chromatographic and adsorption columns [33,34].

Recently, a new family of composite sorbents called selective water sorbents (SWSs) has been presented for sorption cooling and heat pumping [35]. It is based on a porous host matrix (silica, alumina, etc.) and an inorganic salt ($CaCl_2$, LiBr, $MgCl_2$, $MgSO_4$, $Ca(NO_3)_2$, etc.) impregnated inside pores [35–40]. Among the different SWSs, the SWS-1L ("$CaCl_2$ confined to KSK silica gel") shows very high water sorption capacity (up to 0.8 g of water per 1 g of dry adsorbent). This composite adsorbent was synthesized by a dry impregnation of a mesoporous KSK silica gel (average pore size 15 nm) with a saturated aqueous solution of $CaCl_2$ with subsequent drying at 150 °C. The salt content was 33.7 wt.%. Furthermore, according to the SWS-1L water sorption isobars, most of the adsorbed water can be removed at temperatures of 80–100 °C. The thermodynamic performances of SWSs for application in ADCs have been evaluated by means of a lumped mathematical model and compared with those obtained using other adsorbents [41]. The results showed that this new material allows us reaching COP at 0.7–0.8 for basic cooling cycle and 1.4–1.6 for basic heating cycle that is higher than that calculated at the same regeneration temperature (about 95 °C) for micro-porous silica gel + water or 4A zeolite + water pairs. Another important benefit is that the relatively low temperature required for regeneration yields this SWS very attractive for utilization of low grade heat sources, such as solar heat, industrial waste heat, automotive exhaust gas or cascade and tri-generative systems. It should be noted that the dynamic parameters of this adsorbent were studied in [42,43] by an

* Corresponding author. Tel.: +81 92 583 7832; fax: +81 92 583 7833.
E-mail address: bidyutb@cm.kyushu-u.ac.jp (B.B. Saha).

0017-9310/$ - see front matter © 2008 Elsevier Ltd. All rights reserved.
doi:10.1016/j.ijheatmasstransfer.2008.06.018

Nomenclature

Symbol

A	area (m^2)
c_p	specific heat capacity (J/kg K)
h_{fg}	latent heat of evaporation (J/kg)
h	enthalpy/heat transfer coefficient (J/kg, W/m^2 K)
K_o	pre-exponential coefficient (1/Pa)
L	Length (m)
M	mass (kg)
P	pressure (Pa)
R	radial direction (m or mm)
T	temperature (°C)
$\overline{T}$	average temperature (°C)
t	time (s)
u	fluid velocity (m/s)
U	overall heat transfer coefficient (W/m^2 K)
V	volume (m^3)
X	uptake (kg/kg)
Δx	the difference between uptake and off-take during adsorption desorption processes (kg/kg)
Z	axial direction (m or mm)
ρ	density (Kg/m^3)
λ	thermal conductivity (W/m K)
ΔH_{ads}	isosteric heat of adsorption (J/kg)

Subscripts

ads	adsorption
des	desorption
chill	chilled water
fin	fin
ref	refrigerant
cycle	cycle time
f	fluid
M	maximum value
f–m	fluid–metal
m–s	metal–silica gel
fin–s	fin–silica gel
eff	effective value
s	saturation

Superscripts

sg	silica gel
evap	evaporator
cond	condenser
bed	sorption bed
chill	chill water
f	liquid phase
g	gaseous phase
in	inlet
tube	heat exchanger tube
a	adsorbate
cool	cooling fluid
heating	heating fluid

Isothermal Differential Step method [34], and the kinetics of water adsorption on loose silica grains was measured over temperature range of 30–65 °C. It was found that the evolution of the water uptake can be described in terms of the Fickian diffusion model. The apparent water diffusivity in silica pores was calculated and appeared to be close to the Knudsen diffusivity. Basing on the data obtained the specific power of adsorption cooling device was estimated. The adsorption rate for SWS-1L was found to be not less than that for conventional silica Fuji RD used in commercial ADC.

Experimental tests confirmed the promising properties of SWS-1L [41]. It was shown that the use of SWS-1L in the one-bed ADC allowed reaching the cooling *COP* up to 0.6 at the low desorption temperature of 85–90 °C. This was a gross *COP* affected by heat losses, the heat capacity of the inert masses and the heat exchangers efficiency which were not optimized in the unit tested. It was also shown that the low specific power of the tested device is due to the not optimized design of the adsorber heat exchanger as well as to the grain shape of the adsorbent which impedes heat conductivity of the layer. The authors mentioned that both the COP and cooling power are expected to be further improved in the multi-bed system with internal heat recovery and well-designed heat exchanger. The aim of this study was to analyse the performances of SWS-1L in more optimized configuration similar to that used in commercial adsorption chillers. Building from the previous works, this article presents both the steady state and dynamic behaviors of SWS-1L in a two-bed solid sorption cooling system using a transient distributed model. These results are compared with those of commercial adsorption cooler based on silica gel type RD such that a device for new generation of cooling can be enlightened commercially. Both the heat and mass transfer resistances of the adsorption heat exchanger as well as the temporal energetic behavior in the evaporator and condenser are also taken into account in the present model. In this paper, we also elucidated the effects of the isosteric cooling and heating times as well as the total cycle time on the system performances, and demonstrate that the current cooler design tends at optimum conditions.

2. Description of adsorption cooling model

The adsorption chiller which utilizes the adsorbent–adsorbate characteristics and produces the useful cooling effects at the evaporator by the amalgamation of "adsorption-triggered-evaporation" and "desorption-resulted-condensation" was described elsewhere [14–16]. Fig. 1 shows the schematic layout of the adsorption chiller. It comprises an evaporator, a condenser and a pair of reactors or adsorbent beds. For continuous cooling operation, firstly a low-pressure refrigerant (hence water) is evaporated at the evaporator due to external cooling load (or chilled water) and is adsorbed into the solid adsorbent located in the adsorber. The process of adsorption results in the liberation of heat of adsorption at the adsorber providing a useful heat energy output and a cooling effect in the condenser/evaporator heat exchanger. Secondly, the adsorbed bed is heated by the external heat source and the refrigerant is desorbed from the adsorbent and goes to the condenser for condensation by pumping heat through the environment. The condensate (refrigerant) is refluxed back to the evaporator via a pressure reducing valve for maintaining the pressure difference between the condenser and the evaporator. Pool boiling is affected in the evaporator by the vapor uptake at the adsorber, and thus completing the refrigeration close loop or cycle. These phenomena are expressed mathematically using the mass and energy balances between major components of the adsorption chiller system.

2.1. Evaporator

The energy balance becomes

$$\left[(Mc_p)_{eff}^{evap}\right]\frac{dT^{evap}}{dt} = -h_{fg}M^{sg}\frac{dx_{ads}^{bed}}{dt} + h_f M^{sg}\frac{dx_{des}^{bed}}{dt} + (UA)_{chill}\left(\overline{T}^{chill} - T^{evap}\right), \quad (1)$$

Table 1
Summary of adsorbent–refrigerant pairs for cooling applications

Adsorbent–refrigerant pair	System description	Adsorption characteristics	System performance
Silica gel (type A) + water [5,6]	Two-bed adsorption chiller Lumped modelling Experimental investigation	Isotherms: Freundlich's model c^* = 0.346 kg/kg Constant n = 1.6, constant ΔH_{ads} Kinetics: LDF model	A favorable combination has been established for adsorbent-refrigerant pair
Silica gel (type RD) + water [7]	Two-bed adsorption chiller Lumped modeling Experimental investigation	Isotherms: Freundlich's model c^* = 0.552 kg/kg, n = 1.6 constant ΔH_{ads} Kinetics: LDF model	Optimum cooling capacity 1.6 RT. COP values are not given
Silica gel (type RD) + water [8–12]	Adsorption chiller Single-stage Two-stage Three-stage Multi-stage multi-bed duel mode Lumped modelling Experimental analysis	Isotherms: Freundlich's or modified Freundlich's model c^* = 0.346 kg/kg, n = 1.6 Constant ΔH_{ads} Kinetics: LDF model	Cooling capacity and COP have been calculated for different mass flow rates, adsorption/desorption temperatures and cycle periods
Silica gel (type RD) + water [13,14]	Electro-adsorption chiller • Lumped modelling • Experimental investigation	Isotherms: Tóth's model c^* = 0. 45 kg/kg Tóth constant $\tau = 8$ and constant ΔH_{ads} Kinetics: LDF model	Optimum COP is calculated 0.8 for micro-cooling applications
Silica gel (Type RD) + water[15,16]	Two-bed/four-bed adsorption chiller • Lumped modelling • Transient distributed modelling • Experimental investigation	Isotherms: Henry's model Tóth's model c^* = 0. 45 kg/kg Constant $\tau = 8$ Constant ΔH_{ads}	Optimum COP = 0.35 for cooling capacity of 10 kW. The chilled water temperature fluctuations are removed
Silica gel + water [17,18]	• Lumped modelling • Experimental investigation • Heat and mass recovery	Isotherms: Freundlich's model/Dubinin–Astakhov (D–A) isotherm equation, constant ΔH_{ads}. Limiting uptake = 0.346 kg/kg and n = 1.6	COP has been increased 34.4% by heat recovery and 18.3% by mass recovery
Zeolite + water [19–21]	Adsorption cooler Transient distributed 3-D modelling Experimental investigation Account for both internal and external heat and mass transfer	Isotherms: adsorption equilibrium $\ln P = a + b/T$, where a and b depend on the amount of adsorbate c. ΔH_{ads} is calculated as a function of c. Kinetics: linear driving force	COP = 0.45 for $T_{H,in}$ = 300 °C, T_{evap} = 10 °C, T_{cond} = 45 °C
Charcoal (AC35, DEG, NORIT RB, etc.) + methanol, ammonia, etc. carbon + ammonia [22–24]	Adsorption cooling cycle Very simple thermodynamic analysis Performance calculation for adsorbate (ideal gas)	Isotherms: Dubinin–Astakhov/Dubinin–Radushkevich ΔH_{ads} is calculated from Clausius–Clapeyron relations	Overall methanol gives the best COP with 0.5
AC35 + methanol AC35 + ethanol [25] ACF + ethanol [26,27]	Adsorption refrigeration machine • One-dimensional distributed modelling • Annular adsorber • Comparison with experiments	Isotherms: modified Dubinin–Radushkevich equation ΔH_{ads} is calculated as a function of the amount of adsorbate and thermal expansion coefficient of liquid	Not mentioned. For ACF–ethanol system, COP is predicted 0.54 and the size of the bed can be reduced
Carbon + methanol AC + HCFC123/ HCFC124 [28]	Dynamic behavior of adsorption system • Lumped modelling • Adsorbed phase is considered as liquid phase • Experiments	ΔH_{ads} is calculated from Clapeyron equation for perfect gases	COP = 0.29 for regeneration temperature of 125 °C
Zeolite NaX + water activated carbon AX21-ammonia [29,30]	Regenerative heat pump Numerical analysis Simplified distributed modelling Adsorbate is considered as ideal gas	Isotherms: Langmuir model (three terms) for NaX–water pair, and Dubinin equation for AX21-ammonia pair	COP = 0.4 for NaX–water system, and COP = 0.35 for AX21-ammonia system at heat source temp. of 250 °C

Table 1 (*continued*)

Adsorbent–refrigerant pair	System description	Adsorption characteristics	System performance
Zeolite 13X + ammonia zeolite NaX + ammonia AC + ammonia [31,32]	Adsorptive heat pump Distributed two-dimensional modelling Specific heat is considered liquid Showed the thermal conductivity effects on adsorption bed	Isotherms: Dubinin–Radushkevich equation Constant ΔH_{ads}	Optimum COP is calculated 0.8 as a function of thermal conductivity of adsorbent bed

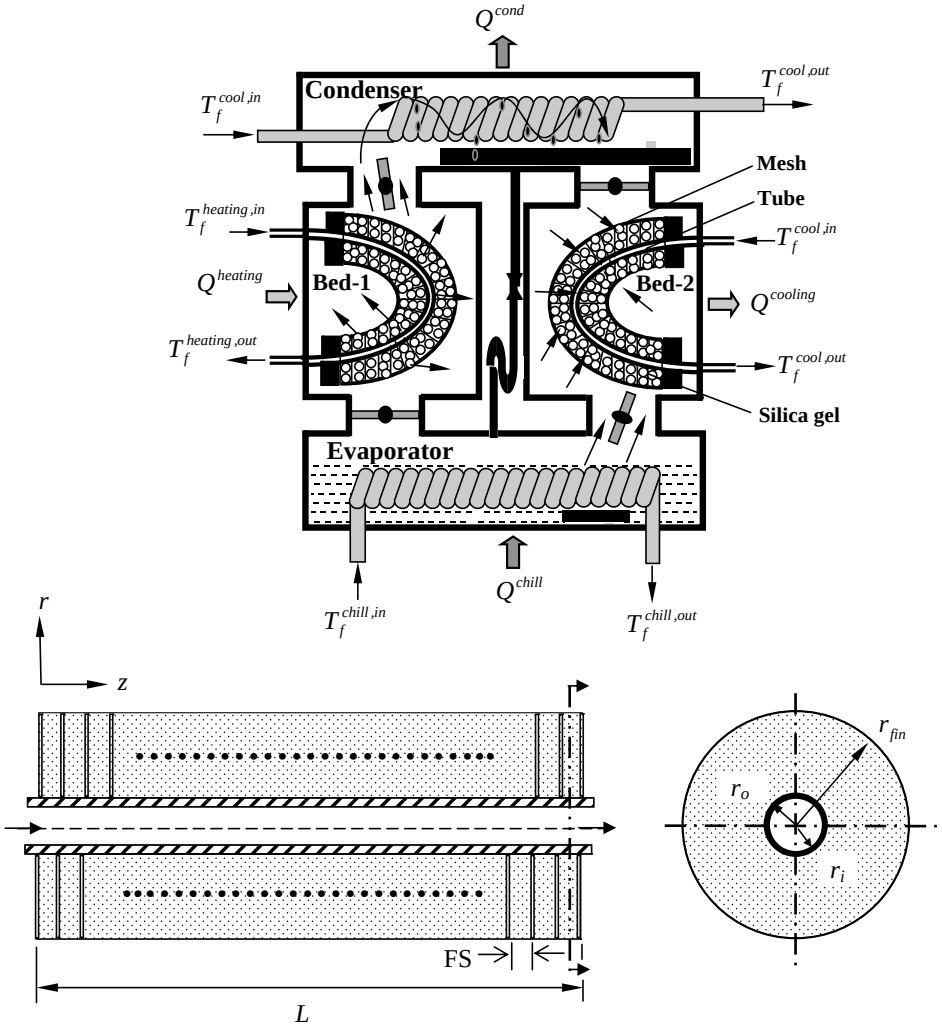

Fig. 1. Schematic of a two-bed adsorption chiller.

where $(Mc_P)^{evap}_{eff}$ is the sum of all mass capacities of the evaporator. The first term on the right hand side defines the latent heat of evaporation that goes to adsorption bed, the second term is the enthalpy of liquid condensate and the last term denotes the cooling capacity of evaporator, which rises from the cooling of chilled water. The energy balance equation on the chilled water control volume is written as

$$\rho_f^{chill} c_{p,f}^{chill} \frac{\partial T^{chill}}{\partial t} = -u_f^{chill} \rho_f^{chill} c_{p,f}^{chill} \frac{\partial T^{chill}}{\partial z} + \lambda_f^{chill} \frac{\partial^2 T^{chill}}{\partial z^2} - \frac{(UA)_{chill}}{V_f^{chill}} (T^{chill} - T^{evap}). \quad (2)$$

Hence the terms, $\frac{dx^{bed}_{ads}}{dt}$ and $\frac{dx^{bed}_{des}}{dt}$ indicate the adsorption rate and the desorption rate. The boundary conditions of the chilled water tube are $T^{chill}(z=0,t) = T^{chill,in}$ and $\frac{\partial T^{chill}}{\partial z}(z = L^{tube}, t) = 0$.

2.2. Adsorption isotherms and kinetics

The adsorption/desorption rate is calculated from the knowledge of adsorption equilibrium and kinetics and is given by the conventional linear driving force (LDF) equation [33]

$$\frac{dx}{dt} = \frac{15 D_{so} e^{-\frac{E_a}{RT}}}{R_p^2} \{x^* - x\}, \quad (3)$$

Table 2
Adsorption isotherms of silica gel + water systems

Type	K_o (Pa^{-1})	ΔH_{ads} (kJ/kg)	x_m (kg kg^{-1})	t_1	Reference
RD (Tóth isotherm)	7.3×10^{-13}	2800	0.4	8	[44,45]
SWS-1 L (Tóth isotherm)	2×10^{-12}	2760	0.8	1.1	Derived from experimental data [46]
Type	a	b	$c \times 10^9$	ΔF kJ/mol	Reference
SWS-1L	2.83378	-3.0133×10^{-4}	7.46702	1–5	[47]
(polynomial equation)	5.80313	−0.00119	69.9054	5–9	[47]

where D_{so} defines a pre-exponential factor of the efficient water diffusivity in the adsorbent, E_a represents the activation energy, R is the universal gas constant and R_p is the average radius of the adsorbent grains. Kinetic data were taken from [42,43]. Hence the adsorption uptake at equilibrium condition is expressed as a function of pressure (P) and temperature (T). The authors have measured the isotherms of water adsorption on silica gel type RD, type A [44,45] and on SWS-1L [46,47]. These experimentally measured data are fitted using the Tóth's equation [48], i.e.,

$$x^* = \frac{x_m K_o \cdot \exp\{\Delta H_{ads}/(R \cdot T)\} \cdot P}{[1 + \{K_o \cdot \exp(\Delta H_{ads}/(R \cdot T)) \cdot P\}^{t_1}]^{1/t_1}}, \quad (4)$$

where x^* is the adsorbed adsorbate at equilibrium conditions, x_m denotes the monolayer capacity, ΔH_{ads} the isosteric enthalpies of adsorption, K_o the pre-exponential constant, and t_1 is the dimensionless Tóth's constant. These values are furnished in Table 2. The most significant difference between these two adsorbents (silica type RD and SWS-1L) lies in their water vapor uptake characteristics. From Table 2, one could observe that the water vapor uptake capacity of SWS-1L is higher than that of type RD. On the other hand, the adsorption uptake of water vapor on SWS-1L is expressed in terms of mole/mole by the polynomial equation, i.e., $x^* = \exp(a + b\Delta F + c\Delta F^2)$ [42,47], where ΔF indicates the Polanyi adsorption potential and is represented by $\Delta F = -RT\ln(P/P_s)$. The values of the adjustable coefficients a, b and c that provide the best approximation of the two segments of the temperature-independent curve of sorption of water by SWS-1L composite [42,47] are also furnished in Table 2. Using these adsorption isotherm data, the conceptual ideal adsorption cooling system developed from type RD silica gel and SWS-1L are shown in Fig. 2. One can also understand from Fig. 2 that the difference between the uptake and off-take $\Delta x\{= x_{ads} - x_{des}\}$ of SWS-1L + water is higher than that of type RD silica gel + water system. It should also be noted here that the values of D_{so}, E_a and R_p are found same for both RD silica gel + water and SWS-1L + water systems, i.e., the adsorption/desorption rate for both systems are nearly same but the difference between the two systems are occurred due to their different uptake capacities.

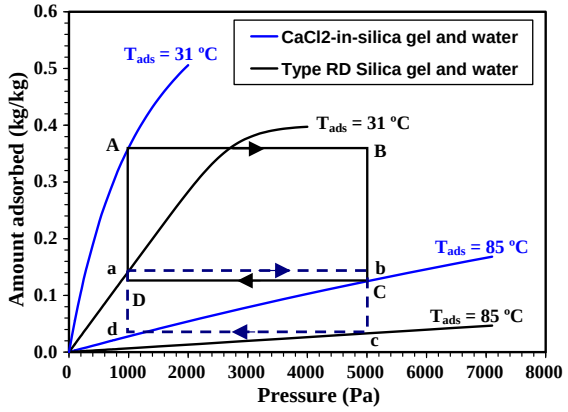

Fig. 2. $P - T - x$ diagram for understanding the conceptual diagram of an adsorption cooling cycle in terms of adsorption uptake against pressure. Here A–B–C–D–A indicates adsorption cooling cycle where SWS-1L and water are used as adsorbent refrigerant pair. In this diagram a–b–c–d–a also defines an adsorption cooling cycle for type RD silica gel and water based system.

2.3. Bed

As the evaporated refrigerant is associated onto the solid adsorbent by the flow of cooling fluid at ambient conditions during adsorption period, and the desorbed refrigerant is dissociated from the solid adsorbent by the flow of heating fluid during desorption period. The heat energy is exchanged between cooling/heating fluid and the adsorption bed. A schematic of the adsorption bed with heat exchanger is shown in Fig. 1. The energy balance for the heat transfer fluid is given by

$$\frac{\partial T_f^j}{\partial t} = -u_f^j \frac{\partial T_f^j}{\partial z} + \frac{\lambda_f^j}{\rho_f^j c_{p,f}^j} \frac{\partial^2 T_f^j}{\partial z^2} - \frac{h_{f-m}^j A_f^j}{\rho_f^j c_{p,f}^j V_f^j}(T_f^j - T_m), \quad (5)$$

where u defines the flow rate of cooling/heating fluid, j indicates heating or cooling for desorption or adsorption, h_{f-m}^j represents the heat transfer coefficient and is calculated from the *Dittus–Boelter* correlation [49]. The boundary condition for fluid flow becomes

during adsorption: $T_f^j(z=0,t) = T_f^{cool,in}$ and $\frac{\partial T_f^j}{\partial z}(z = L^{tube}, t) = 0$,

during desorption: $T_f^j(z=0,t) = T_f^{hot,in}$ and $\frac{\partial T_f^j}{\partial z}(z = L^{tube}, t) = 0$.

The energy balance of the metal tube that contains heat transfer fluid is written as

$$\frac{\partial T^{tube}}{\partial t} = \frac{\lambda^{tube}}{\rho^{tube} c_p^{tube}} \frac{\partial^2 T^{tube}}{\partial z^2} - \frac{h_{f-m}^j A^{tube}}{\rho^{tube} c_p^{tube} V^{tube}} \left(T^{tube} - T_f^j\right) - \frac{h_{m-s} A^{tube}}{\rho^{tube} c_p^{tube} V^{tube}} (T^{tube} - T^{sg}) - \zeta \frac{A^{tube}}{\rho^{tube} c_p^{tube} V^{tube}} \lambda^{fin} \frac{\partial T^{fin}}{\partial r}. \quad (6)$$

Here the value of ς is equal to 1 when any fin is attached with the tube, otherwise $\varsigma = 0$. The boundary conditions of the heat exchanger tube inside the adsorber are $\frac{\partial T^{tube}}{\partial z}(z=0,t) = 0$ and $\frac{\partial T^{tube}}{\partial z}(z = L^{tube}, t) = 0$, respectively.

The fin thickness is very small and the heat transfer in the fin is assumed to be one-dimensional in the radial direction. The energy balance equation of the fin is given by

$$\frac{\partial T^{fin}}{\partial t} = \frac{\lambda^{fin}}{\rho^{fin} c_p^{fin}} \frac{\partial\left(\frac{\partial T^{fin}}{\partial r} r\right)}{r \partial r} - \frac{h_{fin-s} A^{fin}}{\rho^{fin} c_p^{fin} V^{fin}} (T^{fin} - T^{sg}). \quad (7)$$

The boundary conditions are $T^{fin}(r = r_o) = T^{tube}$ and $\frac{\partial T^{fin}}{\partial r}(r = r^{fin}) = 0$.

The energy balance of the adsorbent control volume can be written as (heat flow is considered both in r and z direction)

$$\left(\rho^{sg} c_p^{sg} + \rho^g x c_p^a\right) \frac{\partial T^{sg}}{\partial t} = \nabla.(\lambda^{eff} \nabla T^{sg}) + \rho^{sg} \Delta H_{ads} \frac{dx}{dt} - \frac{h_{fin-s} A^{fin}}{V^{fin}} (T^{fin} - T^{sg}) - \frac{h_{m-s}}{A}^{tube} V^{tube} (T^{tube} - T^{sg}), \quad (8)$$

where the specific heat capacity of the adsorbed phase is given by [50–52] $c_p^a = c_p^g + \Delta H_{ads}\left\{\frac{1}{T^{sg}} - \frac{1}{v^g}\frac{\partial v^g}{\partial T^{sg}}\right\} - \frac{\partial(\Delta H_{ads})}{\partial T^{sg}}$. The first term in the right hand side indicates the specific heat capacity at liquid phase, and the other terms occur due to the non-ideality of gaseous phase, which incorporate two additional inputs from the properties of adsorbent + adsorbate system, namely the ΔH_{ads} and the isotherms $(P-T-x)$ data [50]. On the other hand, the effective thermal conductivity of the adsorbed phase is $\lambda^{eff} = \lambda^g/(\phi + 2/3\frac{\lambda^g}{\lambda^{sg}})$ [34], where ϕ indicates the porosity of bed. Here λ^{eff} is defined as the total thermal conductivity of adsorbent particles stacked together in the adsorber. The boundary condition at radial direction becomes $-\lambda^{eff}\frac{\partial T^{sg}}{\partial r}\big|_{r=r_o} = h_{m-s}(T^{tube} - T^{sg})$ and $\frac{\partial T^{sg}}{\partial r}\big|_{r=r^{fin}} = 0$.

2.4. Condenser

After desorption, the desorbed refrigerant is delivered to the condenser as latent heat and this amount of heat is pumped to the environment by the flow of external cooling fluid. In the modelling, we assume that the condenser tube bank surface is able to hold a certain maximum amount of condensate. Beyond this the condensate would flow into the evaporator via a U-tube. This ensures that the condenser and the desorber are always maintained at the saturated pressure of the refrigerant. The energy balance of the condenser is expressed as

$$\left[(Mc_p)_{eff}^{cond}\right]\frac{dT^{cond}}{dt} = -h_{fg}M^{sg}\frac{dx_{des}^{bed}}{dt} + h_f M^{sg}\frac{dx_{des}^{bed}}{dt} + (UA)^{cond}\left(\overline{T}_f^{cool} - T^{cond}\right), \quad (9)$$

where $(Mc_P)_{eff}^{cond}$ is the sum of all mass capacities of the condenser. The first term on the right hand side defines the latent heat of condensation, the second term is the enthalpy of liquid condensate and the last term denotes the sensible cooling of the condenser. The energy balance equation of the cooling water control volume is written as

$$\rho_f^{cool}c_{p,f}^{cool}\frac{\partial T_f^{cool}}{\partial t} = -u_f^{cool}\rho_f^{cool}c_{p,f}^{cool}\frac{\partial T^{cool}}{\partial z} + \lambda_f^{cool}\frac{\partial^2 T^{cool}}{\partial z^2} - \frac{(UA)^{cool}}{V_f^{cool}}(T^{cool} - T^{cond}). \quad (10)$$

The boundary conditions of the cooled water tube are $T^{cool}(z=0,t) = T^{cool,in}$ and $\frac{\partial T^{cool}}{\partial z}(z = L^{tube}, t) = 0$.

2.5. Mass balance

The mass balance of refrigerant in the adsorption chiller is expressed by

$$\frac{dM_{ref}}{dt} = -M^{sg}\left\{\frac{dx_{des}^{bed}}{dt} + \frac{dx_{ads}^{bed}}{dt}\right\}, \quad (11)$$

where M^{sg} is the mass of adsorbents packed in each of the two adsorbent beds, and M_{ref} is the mass of refrigerant in liquid phase.

The roles of the beds (containing the adsorbent) are refreshed by switching which is performed by reversing the direction of the cooling and the heating fluids to the designated sorption beds and similarly, the evaporator and condenser are also switched to the respective adsorber and desorber. It is noted that during switching interval, no mass transfers occur between the hot bed and the condenser or the cold bed and the evaporator.

The cycle average cooling capacity Q^{chill}, heating capacity $Q^{heating}$ and *COP* are, respectively, calculated as

$$Q^{chill} = \rho_f^{chill}u_f^{chill}A_f^{tube,chill}c_{p,f}^{chill}\int_0^{t_{cycle}}\frac{T_f^{chill,in} - T_f^{chill,out}}{t_{cycle}}dt,$$

$$Q^{heating} = \rho_f^{heating}u_f^{heating}A_f^{tube,bed}c_{p,f}^{heating}\int_0^{t_{cycle}}\frac{T_f^{heating,in} - T_f^{heating,out}}{t_{cycle}}dt,$$

$$\text{and COP} = \frac{Q^{chill}}{Q^{heating}}.$$

3. Results and discussion

The adsorption bed design incorporates a circular finned tube heat exchanger. The values for the parameters used in the present model are furnished in Table 3. Fig. 3 features the temperature histories at the outlets of the type RD (red lines in Fig. 3) and SWS-1L based chiller system (thick black lines in Fig. 3) and these are compared with experimental data (thick blue lines and circles) of type RD silica gel and water based adsorption chiller. Due to the positioning of the temperature sensors, the experimentally measured outlet temperatures are affected by the time constant of downstream mixing valves in the pipeline. It is evident that our present simulation results exhibit a sufficiently good agreement with the experimental data stemming from a distributed parameter model. Fig. 3 also shows the temperature histories at the outlets of the condenser and chilled water. It should be noted here that the delivered chilled water temperature is slightly lower for adsorption chiller employing SWS-1L as can be seen in Fig. 3.

Fig. 4(a) presents the simulated Dühring diagram of the cyclic steady state condition of an entire bed comprising SWS-1L, from which one observes that during cold-to-hot thermal swing of the bed, momentary adsorption takes place although heating source has already been applied to heat up the bed in pre-heating mode. The entire bed is observed to be essentially following an isosteric path (constant x) during switching. In contrast, the local spatial points in the bed are not evolving in an isosteric manner, which is confirmed by the present analysis. This shows that while some parts of the bed may continue to adsorb, other parts desorb, resulting in the entire bed following an isosteric path. At the end of hot-to-cold thermal swing, there is a pressure drop in the bed. This causes the adsorbate in the cool bed to desorb momentarily and condense into the evaporator. The $P-T-x$ diagram for adsorption bed employing RD type silica gel during steady state is also imposed in Fig. 4(b) for comparison.

Table 3
Values adopted for adsorption chiller simulation used in the present model

D_{so}	2.54×10^{-4} m^2/s for SWS-1L and RD silica gel
E_a	4.2×10^4 J/mol for SWS-1L and RD silica gel
R_p	1.7×10^{-4} m for type RD and 1.74×10^{-4} m for SWS-1L
c_p^{sg}	924 J(/kg K)
h_{m-s}	36 W/(m^2 K) [16]
h_{fin-s}	36 W/(m^2 K) [16]
$(UA)^{chill}$	(2557 W/(m^2 K) × 1.37 m^2)
$(UA)^{cond}$	(4115 W/(m^2 K) × 3.71 m^2)
$(Mc_p)_{eff}^{evap}$	(8.9 kg × 386 J/(kg K) + 40 kg × $c_{p,water}$ J/(kg K))
$(Mc_p)_{eff}^{cond}$	(24 kg × 386 J/(kg K) + 5 kg × $c_{p,water}$ J/(kg K))
r_i	7.94 mm
$A^{tube} = 2\pi r_o L^{tube}$	r_o = 8.64 mm, L^{tube} = 1 m
$V_f^{chill} = \pi r_o^2 L^{evap}$	L^{evap} = 2.1 m
$V_f^{cool} = \pi r_o^2 L^{cond}$	L^{cond} = 2.34 m
$V^{fin} = \pi N h(r_{fin}^2 - r_o^2)$	N = 100, h = 0.1 mm, r_{fin} = 22 mm
u_f^{chill}	0.18 m/s
u_f^{cool}	0.198 m/s
$u_f^{heating}$	0.14 m/s
M^{sg}	20 kg
$T_f^{cool,in}$	31 °C
$T_f^{hot,in}$	85 °C
$T_f^{chill,in}$	14.8 °C

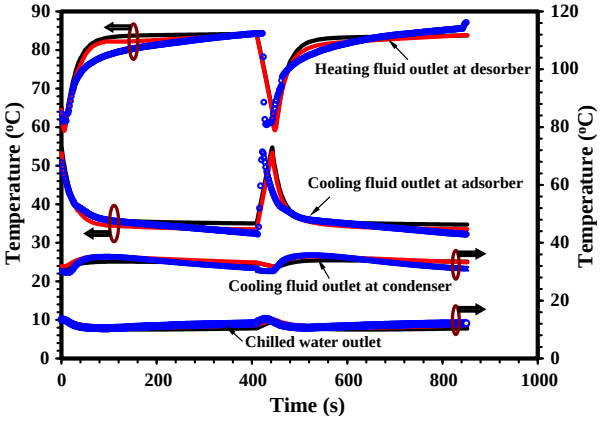

Fig. 3. Simulated (black for SWS-1L + water system; red line for type RD silica gel + water system) and experimental (blue circles for type RD silica gel + water based adsorption system) heating fluid and cooling fluid outlet temperatures from the adsorption chiller system. Simulated and experimentally (for type RD silica gel only) measured fluid outlet temperatures from the condenser and evaporator are also shown here. (For interpretation of the references to color in this figure legend, the reader is referred to the web version of this paper.)

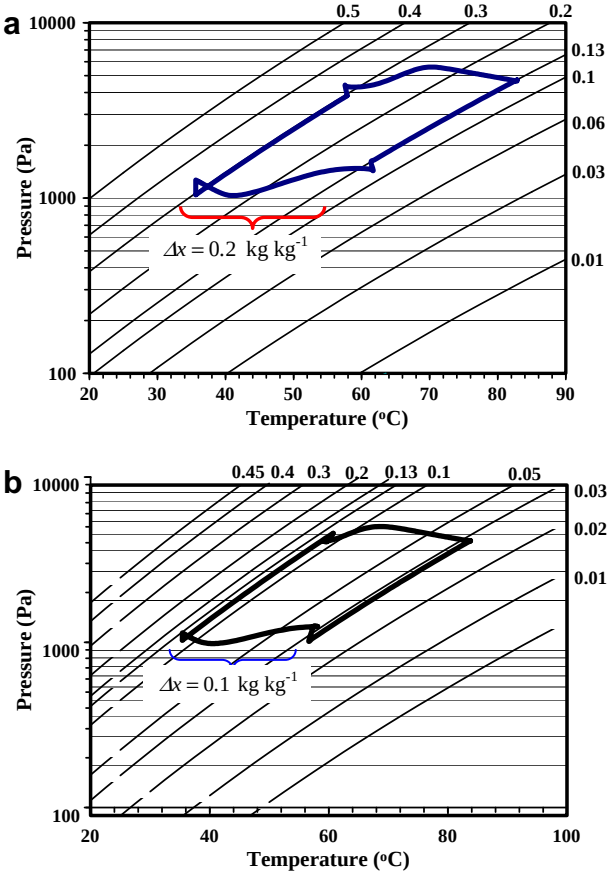

Fig. 4. Dühring diagram of the whole bed under cyclic steady state condition for (a) SWS-1L and water based adsorption chiller, (b) type RD silica gel and water based adsorption cooling cycle.

Fig. 5 presents the effects of cycle time on COP and cycle average chiller cooling capacity for type RD and SWS-1L based adsorption chillers. It is clearly seen that the COP increases monotonically with the cycle time. The reason is that with a longer cycle time, the relative time frame occupied bed switching which involves a

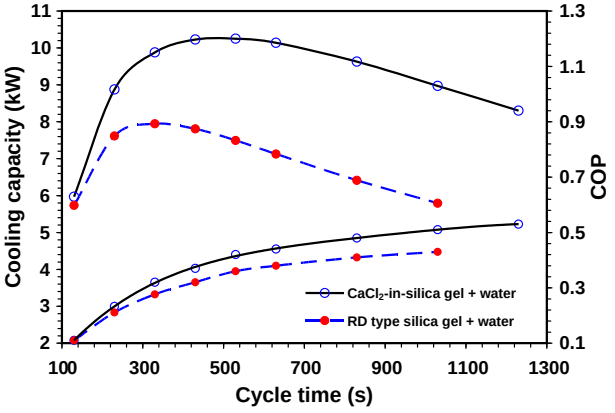

Fig. 5. Effect of cycle time on COP and cycle average cooling capacity.

significant sensible heat exchange is reduced vis-à-vis that of a shorter cycle time. This will lead to a favorable effect on the COP. The variation of cooling capacity is not monotonic. For SWS-1L based adsorption chiller, the cooling capacity increases steeply up to 500 s, and it begins to decrease with a similar slope for cycle time over 500 s. Lower cooling capacity under a relative shorter cycle time is caused by a reduced extent of adsorption, which is also related to a reduced extent of desorption due to the insufficient heating of the desorber. At a certain cycle time, the maximum adsorption/desorption capacity is achieved at the prevailing heating and cooling source temperatures. Extending the cycle time further brings forth unfavorable effect on useful cooling as the cycle

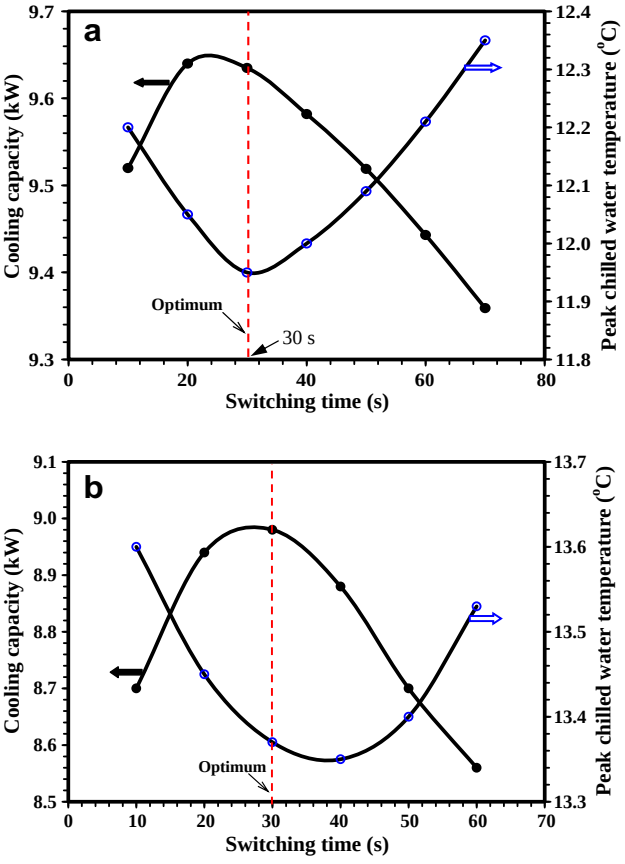

Fig. 6. Effect of switching time on average cooling capacity and peak evaporator chilled water outlet temperature for (a) SWS-1L and water and, (b) type RD silica gel and water systems.

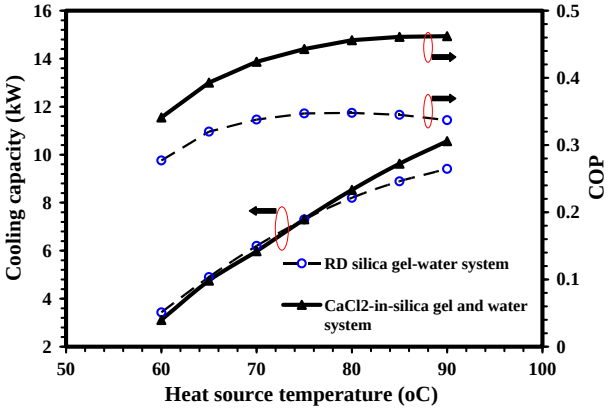

Fig. 7. Influence of driving heat source temperature on cyclic average cooling capacity and COP.

average cooling capacity decreases. For the SWS-1L + water based pair, cycle times longer than 300 s can be realized with higher cooling capacity and COP as compared to the adsorption cooling system based on RD type silica gel + water pair.

When the adsorber or desorber is saturated, the adsorber must be switched to the desorber for regeneration and the desorber must be switched to the adsorber to provide cooling. The switching phase plays an important role on the chiller's performances and may be indispensable. Figs. 6(a) and (b) present the effects of switching time on cycle average cooling capacity and the peak chilled water temperature for SWS-1L + water and RD type silica gel + water systems, respectively. The cycle average cooling capacity varies slightly with switching time and reaches a peak value at 30 s but the maximum chilled water outlet temperature varies significantly with switching time. One can observe that (i) 30 s is the best value for the switching time for SWS-1L and water system as shown in Fig. 6(a), and (ii) 30 s is also the optimum switching time for type RD silica gel + water system [Fig. 6(b)].

The system performance at different driving heat source temperatures in case of optimum conditions [(i) cycle time 420 s, switching time 30 s for type RD silica gel + water system, and (ii) cycle time 630 s, switching time 30 s for SWS-1L + water system] is shown in Fig. 7 for the same heat sink temperature of 31 °C. For type RD silica gel + water system the COP reaches the maximum value of 0.35 at T = 75–80 °C. For SWS-1L + water system at this temperature range the COP is larger (0.42–0.45) and remains almost constant at higher T. The COP of SWS-1L + water system is higher than that of type RD silica gel + water system because of high cooling and less driving heat generation powers, which may occur due to larger Δx for the same heat source and heat sink temperatures. This much larger COP shows significant advantage of the new working pair as compared with the conventional unit. Thus, from the present simulation results, it is found that the newly SWS-1L based adsorption chiller provides a promising unit for cooling applications. This theoretical conclusion should be confirmed practical testing of the new adsorbent in the optimized ADC configuration.

4. Conclusions

We have successfully modeled and predicted the performances of SWS-1L and water based adsorption chiller using a simplified distributed approach such that both the transient and steady state behaviors of ADC can be captured. It is found that the performances of ADC incorporating SWS-1L as adsorbents, in terms of cooling capacity, coefficient of performance and peak chilled water temperature, are better than those of the commercial available silica gel + water based adsorption chiller. An optimum switching time of 30 s is obtained for both cycles and the cycle performance improves with increasing hot water inlet temperature.

References

[1] F. Meunier, Solid sorption: an alternative to CFCs, Heat Recov. Syst. CHP 13 (1993) 289–295.
[2] N.C. Srivastava, I.W. Eames, A review of adsorbents and adsorbates in solid–vapour adsorption heat pump systems, Appl. Therm. Eng. 18 (9–10) (1998) 707–714.
[3] R.E. Critoph, Y. Zhong, Review of trends in solid sorption refrigeration and heat pumping technology, J. Process Mech. Eng. E 219 (2005) 285–300.
[4] L. Yong, K. Sumathy, Review of mathematical investigation on the closed adsorption heat pump and cooling systems, Renew. Sust. Energy Rev. 6 (2002) 305–337.
[5] A. Sakoda, M. Suzuki, Fundamental study on solar powered adsorption cooling system, J. Chem. Eng. Jpn. 17 (1) (1984) 52–57.
[6] A. Sakoda, M. Suzuki, Simultaneous transport of heat and adsorbate in closed type adsorption cooling system utilizing solar heat, J. Solar Energy Eng. Trans. ASME 108 (3) (1986) 239–245.
[7] S.H. Cho, J.N. Kim, Modeling of a silica gel/water adsorption-cooling system, Energy 17 (9) (1992) 829–839.
[8] E.C. Boelman, B.B. Saha, T. Kashiwagi, Experimental investigation of a silica gel–water adsorption refrigeration cycle – the influence of operating conditions on cooling output and COP, ASHRAE Trans. 101 (2) (1995) 358–366.
[9] B.B. Saha, E.C. Boelman, T. Kashiwagi, Computer simulation of a silica gel–water adsorption refrigeration cycle – the influence of operating conditions on cooling output and COP, ASHRAE Trans. 101 (2) (1995) 348–357.
[10] B.B. Saha, A. Akisawa, T. Kashiwagi, Solar/waste heat driven two-stage adsorption chiller: the prototype, Renew. Energy 23 (1) (2001) 93–101.
[11] B.B. Saha, A. Chakraborty, S. Koyama, K. Srinivasan, K.C. Ng, T. Kashiwagi, P. Dutta, Thermodynamic formalism of minimum heat source temperature for driving advanced adsorption cooling device, Appl. Phys. Lett. 91 (2007) 111902.
[12] B.B. Saha, S. Koyama, J.B. Lee, K. Kuwahara, K.C.A. Alam, Y. Hamamoto, A. Akisawa, T. Kashiwagi, Performance evaluation of a low-temperature waste heat driven multi-bed adsorption chiller, Int. J. Multiphase Flow 29 (8) (2003) 1249–1263.
[13] K.C. Ng, M.A. Sai, A. Chakraborty, B.B. Saha, S. Koyama, The electro-adsorption chiller: performance rating of a novel miniaturized cooling cycle for electronics cooling, J. Heat Transf. 128 (9) (2006) 889–896.
[14] B.B. Saha, A. Chakraborty, S. Koyama, K.C. Ng, M.A. Sai, Performance modelling of an electro-adsorption chiller, Philos. Mag. 86 (23) (2006) 3613–3632.
[15] H.T. Chua, K.C. Ng, A. Malek, T. Kashiwagi, A. Akisawa, B.B. Saha, Multi-bed regenerative adsorption chiller – improving the utilization of waste heat and reducing the chilled water outlet temperature fluctuation, Int. J. Refrig. 24 (2) (2001) 124–136.
[16] H.T. Chua, K.C. Ng, W. Wang, C. Yap, X.L. Wang, Transient modeling of a two-bed silica gel–water adsorption chiller, Int. J. Heat Mass Transf. 47 (4) (2004) 659–669.
[17] Y.L. Liu, R.Z. Wang, Z.Z. Xia, Experimental performance of a silica gel–water adsorption chiller, Appl. Therm. Eng. 25 (2005) 359–375.
[18] D.C. Wang, Z.Z. Xia, J.Y. Wu, R.Z. Wang, H. Zhai, W.D. Dou, Study of a novel silica gel–water adsorption chiller: part I. Design and performance prediction, Int. J. Refrig. 28 (7) (2005) 1073–1083.
[19] L.Z. Zhang, L. Wang, Effects of coupled heat and mass transfers in adsorbent on the performance of a waste heat adsorption cooling unit, Appl. Therm. Eng. 19 (2) (1999) 195–215.
[20] L.Z. Zhang, L. Wang, Momentum and heat transfer in the adsorbent of a waste-heat adsorption cooling system, Energy 24 (7) (1999) 605–624.
[21] L.Z. Zhang, A three-dimensional non-equilibrium model for an intermittent adsorption cooling system, Solar Energy 69 (1) (2000) 27–35.
[22] R.E. Critoph, Performance limitations of adsorption cycles for solar cooling, Solar Energy 41 (1) (1988) 21–31.
[23] R.E. Critoph, Forced convection adsorption cycles, Appl. Therm. Eng. 18 (9–10) (1998) 799–807.
[24] R.E. Critoph, Simulation of a continuous multiple-bed regenerative adsorption cycle, Int. J. Refrig. 24 (5) (2001) 428–437.
[25] L. Luo, D. Tondeur, Transient thermal study of an adsorption refrigerating machine, Adsorption 6 (1) (2000) 93–104.
[26] B.B. Saha, I.I. El-Sharkawy, A. Chakraborty, S. Koyama, Study on an activated carbon fiber-ethanol adsorption chiller: part I – system description and modelling, Int. J. Refrig. 30 (1) (2007) 86–95.
[27] B.B. Saha, I.I. El-Sharkawy, A. Chakraborty, S. Koyama, Study on an activated carbon fiber-ethanol adsorption chiller: part II – performance evaluation, Int. J. Refrig. 30 (1) (2007) 96–102.
[28] S.M. Sami, C. Tribes, An improved model for predicting the dynamic behaviour of adsorption systems, Appl. Therm. Eng. 16 (2) (1996) 149–161.
[29] N.B. Amar, L.M. Sun, F. Meunier, Numerical analysis of adsorptive temperature wave regenerative heat pump, Appl. Therm. Eng. 16 (5) (1996) 405–418.
[30] G. Cacciola, G. Restuccia, Reversible adsorption heat pump: a thermodynamic model, Int. J. Refrig. 18 (2) (1995) 100–106.

[31] L.M. Sun, N.B. Amar, F. Meunier, Numerical study on coupled heat and mass transfers in an adsorber with external fluid heating, Heat Recov. Syst. CHP 15 (1) (1995) 19–29.
[32] L.M. Sun, Y. Feng, M. Pons, Numerical investigation of adsorptive heat pump systems with thermal wave heat regeneration under uniform-pressure conditions, Int. J. Heat Mass Transf. 40 (2) (1997) 281–292.
[33] E. Glueckauf, Formulae for diffusion into spheres and their application to chromatography, Trans. Faraday Soc. 51 (1955) 1540–1551.
[34] D.M. Ruthven, Principles of Adsorption and Adsorption Processes, London, John Wiley & Sons, 1984.
[35] Y.I. Aristov, G. Restuccia, G. Cacciola, V.N. Parmon, A family of new working materials for solid sorption air conditioning systems, Appl. Therm. Eng. 22 (2) (2002) 191–204.
[36] Y.I. Aristov, New composite adsorbents for conversion and storage of low temperature heat: activity in the Boreskov Institute of Catalysis, J. Heat Transf. Soc. Jpn. 45 (192) (2006) 12–19.
[37] Y.I. Aristov, New family of materials for adsorption cooling: material scientist approach, J. Eng. Thermophys. 16 (2) (2007) 63–72.
[38] I.A. Simonova, Y.I. Aristov, Sorption properties of calcium nitrate dispersed in silica gel: the effect of pore size, Russ. J. Phys. Chem. 79 (8) (2006) 1307–1311.
[39] Y.I. Aristov, L.L. Vasiliev, New composite sorbents of water and ammonia for chemical and adsorption heat pumps (review), J. Eng. Thermophys. 79 (6) (2006) 1214–1229.
[40] L.G. Gordeeva, E.V. Savchenko, I.S. Glaznev, V.V. Malakhov, Y.I. Aristov, Impact of phase composition on water adsorption on inorganic hybrides salt/silica, J. Colloid Interface Sci. 301 (2006) 685–691.
[41] G. Restuccia, A. Freni, S. Vasta, Y.I. Aristov, Selective water sorbent for solid sorption chiller: experimental results and modelling, Int. J. Refrig. 27 (2004) 284–293.
[42] Y.I. Aristov, M.M. Tokarev, A. Freni, G. Restuccia, Comparative study of water adsorption on SWS-1L and microporous silica: equilibrium and kinetics, in: Proc. Sorption Heat Pumps Conference, Denver, USA, 2006 (CD-ROM).
[43] Y.I. Aristov, I.S. Glaznev, A. Freni, G. Restuccia, Kinetics of water sorption on SWS-1L (calcium chloride confined to mesoporous silica gel): influence of grain size and temperature, Chem. Eng. Sci. 61 (2006) 1453–1458.
[44] A. Chakraborty, Thermoelectric Cooling Devices: Thermodynamic Modelling and Their Applications in Adsorption Cooling Cycles, Ph.D. Thesis, National University of Singapore, November 2005.
[45] H.T. Chua, K.C. Ng, A. Chakraborty, N.M. Oo, M.A. Othman, Adsorption characteristics of silica gel + water systems, J. Chem. Eng. Data 47 (5) (2002) 1177–1181.
[46] Y.I. Aristov, M.M. Tokarev, G. Cacciola, G. Restuccia, Selective water sorbents for multiple applications: 1. $CaCl_2$ confined in mesopores of the silica gel: sorption properties, React. Kinet. Catal. Lett. 59 (2) (1996) 325–334.
[47] M.M. Tokarev, B.N. Okunev, M.S. Safonov, L.I. Kheifets, Y.I. Aristov, Approximation equations for describing the sorption equilibrium between water vapor and a SWS-1L composite sorbent, Russ. J. Phys. Chem. 79 (9) (2005) 1490–1493.
[48] J. Tóth, State equations of the solid–gas interface layers, Acta Chem. Acad. Sci. Hung. 69 (1971) 311–338.
[49] J.P. Holman, Heat Transfer, nineth ed., McGraw-Hill Book, 2002.
[50] A. Chakraborty, B.B. Saha, S. Koyama, K.C. Ng, The specific heat capacity of a single component adsorbent–adsorbate system, Appl. Phys. Lett. 90 (2007) 171902.
[51] A. Chakraborty, B.B. Saha, S. Koyama, K.C. Ng, On the thermodynamic modeling of isosteric heat of adsorption and comparison with experiments, Appl. Phys. Lett. 89 (2006) 171901.
[52] Y.I. Aristov, M.M. Tokarev, G. Cacciola, G. Rectuccia, Properties of the system "calcium chloride–water" confined in pores of the silica gel: specific heat thermal conductivity, Russ. J. Phys. Chem. 71 (3) (1997) 391–394.